ELSEVIER

Journal of Molecular Catalysis A: Chemical 172 (2001) 67–80

JOURNAL OF MOLECULAR CATALYSIS A: CHEMICAL

www.elsevier.com/locate/molcata

Synchrotron XAS studies on a half-sandwich titanium-based polyethylene catalyst

Eric P. Wasserman [a,*], Alistair D. Westwood [a], Zhengtian Yu [a], John H. Oskam [b], Susan L. Duenas [a]

[a] *Union Carbide Corporation, Polyolefins Research and Development, P.O. Box 670, Bound Brook, NJ 08805, USA*

[b] *Univation Technologies, P.O. Box 670, Bound Brook, NJ 08805, USA*

Received 4 January 2001; received in revised form 5 March 2001; accepted 5 March 2001

Abstract

A new catalyst for the copolymerization of ethylene and α-olefins, based on (η^5-C_5Me_5)$TiCl_3$, methanol, 2,6-di-*t*-butylphenol, and methylaluminoxane, is described. The polymerization behavior indicates the necessity of the hindered phenol for high activity, but does not prove that a phenoxide group exists in the coordination sphere of the active site. The titanium K-edge EXAFS spectra of mixtures of various combinations of the four components are best fit to a structure containing a short Ti–O bond, a Ti–arene interaction, and two alkyl carbons. XANES, and to a lesser extent X-ray photoelectron spectroscopy (XPS), spectra show that the presence of the alcohol(s) in the catalyst is correlated with higher titanium absorption energies as well as narrower peak widths.

Keywords: EXAFS; XANES; Olefin polymerization; Aluminoxane

1. Introduction

Structural elucidation of aluminoxane-activated polyolefin catalysts is made difficult by the heterogeneity of the cocatalyst. To our knowledge, no adduct from the reaction of an aluminoxane and a organometallic catalyst precursor has been characterized by X-ray crystallography. Recently, O'Hare and co-workers demonstrated [1] the utility of EXAFS spectroscopy as a tool in deriving structural information from a mixture of methylaluminoxane (MAO) and the metallocene *rac*-Et(Ind)$_2$ZrCl_2 contained in the pores of MCM-41. This work and other EXAFS studies on polymerization systems [2–5] led us to employ Ti K-edge EXAFS to gain insights into the atomic environment around the transition metal atom in a half-sandwich titanium-based polyolefin catalyst.

The catalyst chosen for this study is formed from a mixture of four components: pentamethylcyclopentadienyltitanium trichloride (Cp^*TiCl_3, $Cp^* = C_5Me_5$), methanol, 2,6-di-*t*-butylphenol (DTBP), and MAO [6].[1] Examples of the catalytic behavior of this system are summarized in Table 1. The catalysts containing DTBP copolymerize ethylene and 1-hexene with high activity; these systems also possess low rates of chain transfer and a relatively small preference for the incorporation of ethylene over the larger

[1] Both methanol and DTBP were found to be important in achieving high activity while producing compositionally homogeneous ethylene/α-olefin copolymers; the ratios of components chosen for this study reflect those employed in the patent examples.

* Corresponding author.

1381-1169/01/$ – see front matter
PII: S1381-1169(01)00126-1

Table 1
Ethylene–1-hexene copolymerizations[a] using Cp^*TiCl_3-based catalysts

MeOH/Ti	DTBP/Ti	Yield (g)	1-Hexene content (mol%)	M_w/1000	M_w/M_n	T_m (°C)	ΔH_f[b]
0	0	0.7	14.9	179.1	3.5	122.1	0.42
4	0	1.0	13.6	173.9	3.4	117.7	0.11
0	100	76.6	13.9	160.8	2.9	n.f.[c]	0
4	100	73.1	14.2	156.4	2.9	n.f.	0

[a] Conditions: 80°C; 2.5 μmol Ti; 1.25 mmol Al (MAO); 100±2 psi (total); 50 cm^3 1-hexene; 600 cm^3 hexanes; MeOH quench after 0.5 h.
[b] Heat of fusion, second heating (cal/g).
[c] n.f.: Not found.

comonomer. In these aspects, the polymerizations resemble those by a recently described catalyst based on $Cp^*Ti(OAr)Cl_2$ (Ar = 2,6-diisopropylphenyl) and MAO [7]. The active site of this catalyst is presumed to retain the metal phenoxide linkage during chain propagation. Does a similar Ti–OAr bond exist in the activated catalyst made from the four components described above?

The role played by DTBP in this catalyst is not straightforward. In Table 1, one notes a similar level of hexene incorporation by the three-component mixture lacking DTBP as in that with DTBP, although at a pronounced loss in polymerization activity. The differential scanning calorimetry (DSC) data indicate that, while the overall level of 1-hexene incorporation remains high, highly crystalline material melting above 90°C appears in polymers produced in the absence of DTBP (Fig. 1). (This effect is somewhat diminished by the presence of MeOH).[2] Given the low level of total crystallinity, even in the entirely alcohol-free run, it is reasonable to postulate that a second type of site with substantially higher selectivity for ethylene insertion contributes polymer in the DTBP-free runs. The data also imply that the sites responsible for the overall high hexene levels in the polymer continue to function even without DTBP. The hindered phenol clearly enables the catalyst to attain high activity. The retention of basic kinetic parameters such as monomer reactivity ratio and chain-transfer rate by the DTBP-free catalysts argues against the existence of a Ti–OAr (Ar = 2,6-di-*t*-butylphenyl) bond in one formulation and not in the others.

The X-ray techniques discussed herein are potentially powerful tools in the study of amorphous organometallic catalysts. Practical considerations of signal-to-noise (S/N), however, may require that the samples subjected to analysis be enriched in the transition metal under study. For this study, the ratios of MAO and DTBP to titanium were considerably lower (by a factor of 25–40) than in the polymerization runs shown in Table 1. (The relative ratio of DTBP to MAO was roughly the same as in Table 1, however). This difference in catalyst composition between its application in polymerization and its spectroscopic interrogation will necessarily limit the extent to which the conclusions drawn from the X-ray analysis can

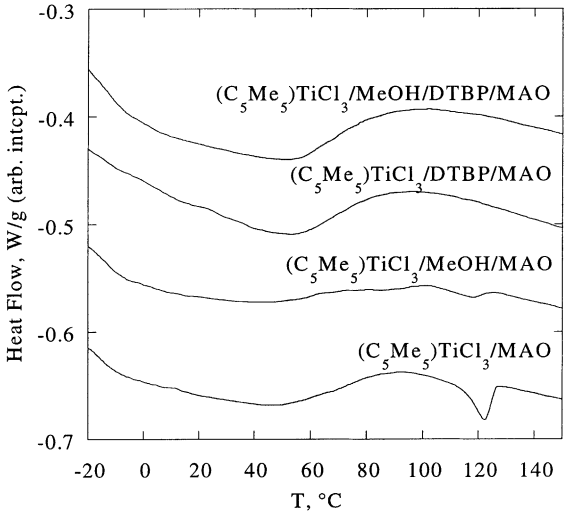

Fig. 1. DSC traces for copolymers from ethylene–1-hexene copolymerizations (see Table 1).

[2] While the role of methanol appears to be slight in the polymerization data presented herein, it has been found to be important to maintaining the compositional homogeneity of EPDM produced by this catalyst system: cf. [6].

be understood to apply to solution polymerization conditions.

2. Experimental

2.1. Materials

Pentamethylcyclopentadienyltitanium trichloride (Cp^*TiCl_3) was obtained from Strem Chemical and used without further purification. Methanol (Fisher, HPLC grade) was passed through alumina and sparged with nitrogen. Toluene was stored over sodium–potassium alloy and filtered through activated alumina under nitrogen and stored in the drybox. 1-Hexene (Alfa Aesar, ≥98%) was passed through alumina and sparged with nitrogen. Ethylene (polymer grade, 99.9%) was passed through dried 13X molecular sieves. Hexanes were "high purity grade" (85% *n*-hexane), and passed through dry molecular sieves and sparged with nitrogen prior to use. Boron nitride and DTBP were obtained from Aldrich Chemical and used as received. MAO was purchased from Albemarle as a 3.15 mol/l solution in toluene.

2.2. Polymerization

Polymerizations were conducted in a chrome-plated, stainless steel autoclave (Fluitron, Ivyland, PA) containing a baffle assembly, agitated at 800 rpm using a magnetically-driven impeller. A solution of Cp^*TiCl_3 (and optionally MeOH) in toluene (2.5 μmol Ti) was injected via syringe at final reactor pressure after the reactor was filled with 600 cm^3 hexanes and 50 cm^3 1-hexene, and MAO and brought to 60°C. After injection, the reaction temperature set point was reset to 80°C and this temperature was maintained for the remainder of the run. The reactor was run for 0.5 h with temperature controlled by steam–water mixtures dictated by a computer-driven P–I–D system. Polymerization was terminated by injection of 1 cm^3 methanol.

2.3. DSC

DSC thermographs were generated on polymer samples of approximately 10 mg using a TA 2920 calorimeter (TA Instruments, Inc.). DSC data reported in this paper were taken from the second heating cycle, 10°C/min heating rate.

2.4. Size-exclusion chromatography (SEC)

MW and MWD of polymers were measured by a Waters 150C GPC and/or a Polymer Laboratories PL-210 GPC equipped with three Showa Denko Showdex GPC AT-806MS 10 μ mixed-bed columns and one Phenogel 10 μ, 50 Å column, operating at 140°C with 1,2,4-trichlorobenzene as the solvent and mobile phase at flow rate of 1 cm^3/min. The sample injection size is 0.3 cm^3 of polymer solution at concentration of 0.1% w/v. The actual molecular weight statistics such as weight average MW and number average MW are derived from a calibration that is obtained with a polyethylene standard, SRM-1496, available from the National Institute of Standards Technology. The weight average molecular weight of SRM-1496 was determined by static light scattering to be 190,000 g/mol. The number average molecular weight was determined by ^{13}C NMR end-group analysis to be 15,700 g/mol.

2.5. 1-Hexene content analysis by ^{13}C NMR

All samples were prepared by dissolving polymer in *o*-dichlorobenzene to achieve a final concentration of 8% (w/v). ^{13}C NMR spectra were acquired at 115°C on a Bruker AC-300 NMR spectrometer using NOE enhanced conditions with a 30° PW and a 5 s repetition time. The number of scans was usually about 1000. The area of the peaks was measured along with the area of the total aliphatic region. The areas of carbons contributed by the comonomer were averaged and ratioed to the area of the backbone to give the mole fraction comonomer.

2.6. XAS sample preparation

All sample handling was done under nitrogen. For sample 1 (Table 2), the compound was merely ground in a mortar and pestle. For the other materials, a solution of Cp^*TiCl_3 was dissolved in toluene, and premixed at room temperature with a solution of methanol (MeOH) (when called for) for at least 30 min. A similar mixture of DTBP and MAO was prepared by stirring toluene solutions of the two (when called for) for at least 30 min at room temperature. The solution of MAO (and optionally DTBP) was mixed with the solution of Cp^*TiCl_3 (and optionally

Table 2
ESCA Binding energies[a] and peak widths for Ti $2p^{3/2}$ as a function of catalyst composition

Sample (molar ratios)	Energy (eV)	Width (eV)
Cp^*TiCl_3/MAO (1:13)	458.75 ± 0.18	2.46 ± 0.58
Cp^*TiCl_3/MeOH/MAO (1:3:13)	459.48 ± 0.34	2.63 ± 0.26
Cp^*TiCl_3/DTBP/MAO (1:5:13)	459.22 ± 0.26	2.04 ± 0.28
Cp^*TiCl_3/MeOH/DTBP/MAO (1:3:5:13)	459.19 ± 0.26	2.12 ± 0.28

[a] With 2σ error bars.

MeOH) for about 30 min at room temperature, then reduced in vacuo to a solid by heating in an oil bath set to 40–60°C for 2–3 h. The solids were then scraped out and ground to a fine powder in a mortar and pestle. The powders were then sealed in glass ampules under vacuum and shipped. Prior to placement in the sample holder, the samples were removed from the ampule and ground again in a mortar and pestle (optionally with boron nitride). The initial aim of the dilution was to provide transmission of approximately 30% of the light, however, it was not always practical to achieve this and good S/N because much of the light absorption came from heavy non-titanium atoms such as Cl and Al. Each sample cell was first sealed on one side with either polyimide (Kapton®) tape (0.5 mm, with 0.5 mm silicone adhesive), or with cellulose acetate (Scotch™) tape.

2.7. Synchrotron XAS

The experiments done at SSRL were performed on beamline 2–3 of SPEAR. A Si(2 2 0) double crystal monochromator, detuned so that throughput was cut by 50% from its maximum to better reject unwanted harmonics, was employed. Spectra were obtained from the data averaging of from 3 to 12 scans, each scan containing 300–350 data points distributed at highest density in the XANES region, at lower density in the high-energy end of the EXAFS region, and at lowest density in the region preceding the sample pre-edge features. Initial data workup (data averaging, background removal, de-glitching) employed the analysis package EXAFSPAK (Drs. G.N. George and I.J. Pickering, SSRL).

A titanium metal foil placed along the beam axis after the sample cell provided the frequency reference. The beam path was continuously purged with purified helium excepting the chamber containing the titanium foil reference, which was purged with argon. Spectra were acquired at ambient temperature. The beam size was 1–2 mm high and approximately 5 mm wide; absorption was estimated from fluorescence. The sample cell holder was mounted at a 45° angle to the beam so that its fluorescence would be collected by the Lytle detector on the perpendicular axis. The overall X-ray absorption was generally between 20 and 80% of incident intensity. Both direct and indirect (fluorescence) absorption spectra were simultaneously obtained. The fluorescence-derived spectra were judged to be less subject to artifacts due to strong absorption and uneven sample thickness, and were therefore used in the analysis.

The bulk of the data workup was done at Bound Brook, either using a home copy of EXAFSPAK or MSI Cerius^2 (EXAFS, vide infra).[3] XANES spectra were fit to combinations of several peaks, one step function, and baseline correction functions using the EDGFIT module of EXAFSPAK. XANES pre-edge peaks were fit to 1:1 mixed Gaussian/Lorentzian lineshapes. All the EXAFS simulations were carried out by using Cerius^2/EXAFS package (version 3.9), using curved-wave theory, at the single-scattering level. Phase shifts for each type of the atom were computed based on the von Barth method.

2.8. XPS

XPS measures the binding energies of core and valence level electrons from atoms comprising the surface [19], these energies being sensitive to the atomic environment of its host atom. The Ti $2p^{3/2}$ (L_{III}) peak and Ti $2p^{1/2}$ (L_{II}) peak at around 454 and 460 eV, respectively, corresponding to the 2p electron orbitals, were utilized in the study.

[3] The Cerius^2 EXAFS module incorporates the EXCURV92 program developed at EPSRC Daresbury Laboratory by Binsted et al. in 1991.

Samples were prepared in the same manner as for the synchrotron XAS samples. All samples were run on a Surface Science Laboratories Inc. SSX-100 XPS spectrometer.[4] A monochromatic aluminum X-ray source, Al Kα = 1.486 keV, was used for the analysis. Samples were pressed into a piece of paraffin tape and then attached to a copper block using double-sided tape, with the copper block then being mounted on the XPS stage using double-sided tape to ensure that the samples were fully floating. A flood gun operating at 2 eV was used for charge compensation. The technique relies on an internal reference which is typically taken as adventitious adsorbed hydrocarbons on the sample surface. Initially, a gold-coated silicon wafer was tried with the catalysts deposited on the gold surface, with the gold acting as the reference material. Unfortunately, significant differential charging occurred between the sample and gold-coated wafer. In place of the gold, paraffin film, which provided an excess amount of C–C bonds at 284.6 eV, provided the reference binding energy.

Survey scans from 0 to 1100 eV binding energy were conducted with a pass energy of 150 eV, 6–12 scans and a spot size of 1000 μm. Survey scans allowed an overall view of the surface. In order to accurately measure small changes in the binding energy of the Ti $2p^{3/2}$ peak high resolution scans across the titanium region were required. All high resolution spectra required analysis of the carbon region in order to charge correct the titanium region. Typical analysis parameters for the carbon region were a 30 eV window, 20 scans, and for the titanium region, a 30 eV window, 250 scans, and all were obtained using a pass energy of 50 eV and a spot size of 600 μm.

3. Results and discussion

3.1. X-ray photoelectron spectroscopy (XPS)

XPS, a tool complementary to K-edge X-ray spectroscopy, was used to characterize mixtures of catalyst components in an attempt to find correlations with catalyst performance. The binding energies of the Ti $2p^{3/2}$ peak for various catalyst mixtures are shown in Table 2. The binding energy for Cp^*TiCl_3 could not be obtained because the sample sublimed in the deep vacuum conditions of the XPS setup. Therefore, the only effect that could be investigated was that of the two alcohols on the MAO-activated precursor. The values of the Ti $2p^{3/2}$ binding energy in the mixtures are consistent with a formal Ti(IV) oxidation state [8], rather than Ti(III).[5] The presence of MeOH or DTBP causes an increase in the Ti $2p^{3/2}$ binding energy by less than one electron volt. This is consistent with a reduction of the electron density around the Ti atom. The Ti $2p^{3/2}$ peaks for the samples containing DTBP were narrower than for those without; this narrowing can be attributed to greater homogeneity among titanium environments [9,10]. To the extent that greater electrophilicity and site homogeneity can be associated with highly-active, homogeneous olefin polymerization catalysts, these data are broadly consistent with the polymerization data in Table 1.

Table 3
Constitution of samples[a] analyzed by synchrotron XAS

Sample	MeOH/Ti	DTBP/Ti	Al/Ti	BN[b]
1	0	0	0	80
2	0	0	18	50
3	3	0	18	60
4	0	6	18	0
5	3	6	18	50

[a] Transition metal component: Cp^*TiCl_3; other components described in molar ratios to Cp^*TiCl_3.
[b] Boron nitride in sample prepared for spectroscopy (wt.%).

3.2. XANES

To gain deeper insight into the nature of the active site of this catalyst, various combinations of the four components were subjected to Ti K-edge XAS analysis at the Stanford Synchrotron Radiation Laboratory (SSRL). The compositions of the interrogated mixtures are listed in Table 3, and include samples with precursor alone (sample 1), as well as various

[4] Surface Science Laboratories, no longer in existence. All service, maintenance, and upgrades performed by Service Physics, Los Altos, CA.

[5] Although it should be mentioned that a previous study in our laboratory showed Cp_2TiCl_2 to have a Ti $2p^{3/2}$ binding energy of 457.1 ± 0.1 eV indicating that titanocene had an electronic environment similar to the Ti(III) ions in Ti_2O_3. The FWHM of the Ti $2p^{3/2}$ peak was 1.6 eV.

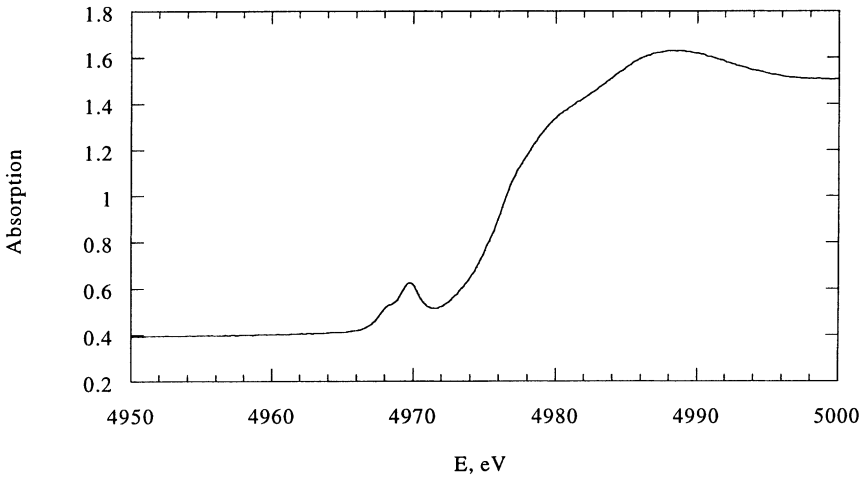

Fig. 2. XANES spectrum of sample 5.

combinations of alcohol(s) and MAO. Boron nitride was occasionally used as a diluent. Data collection in the 50 eV window about the K-edge for our samples gave the XANES spectra; one such spectrum, that of the four-component catalyst, is shown in Fig. 2. We also found the edge energy E_0, which is part of the XANES peak-fitting output, to vary significantly not only from sample to sample, but from fit to fit on a single sample. We therefore restrict our discussion to the (generally) well-resolved pre-edge features at 4967 and 4969 eV, shown for three samples in Fig. 3. The energies and widths for these peaks are displayed in Figs. 4 and 5, respectively.

If the values for the peak energies, heights, and widths which result from curve-fitting of these pre-edge features reflect changes in catalyst structure and homogeneity, then we can draw some interesting conclusions about the roles of the different components of the catalyst. First, when comparing the peak energies (Fig. 4), we note that the peak positions generally increase in energy as one adds the alcohols. This correlates with improved catalyst activity

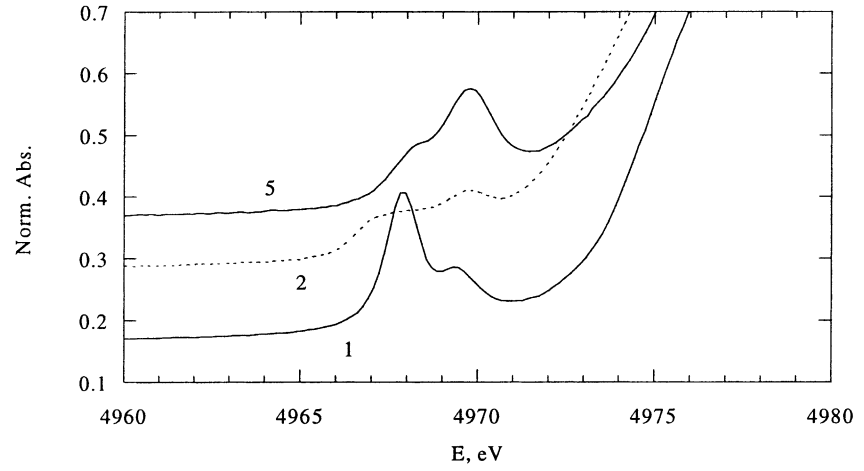

Fig. 3. Comparison of pre-edge features for samples 1, 2 and 5.

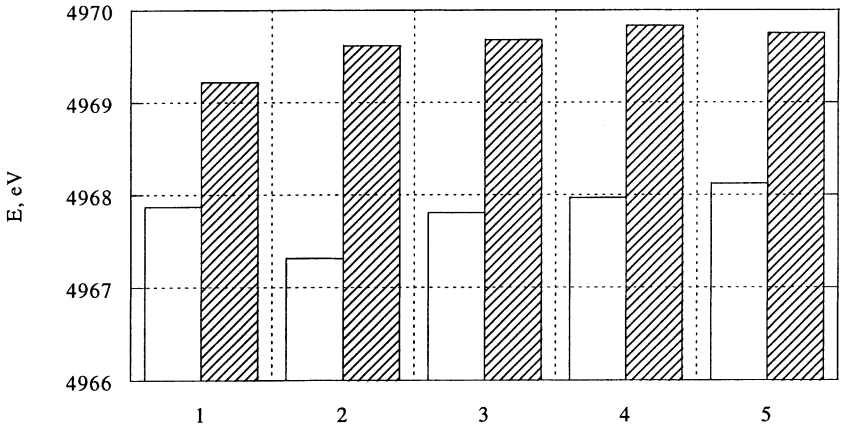

Fig. 4. XANES pre-edge energies for samples 1–5.

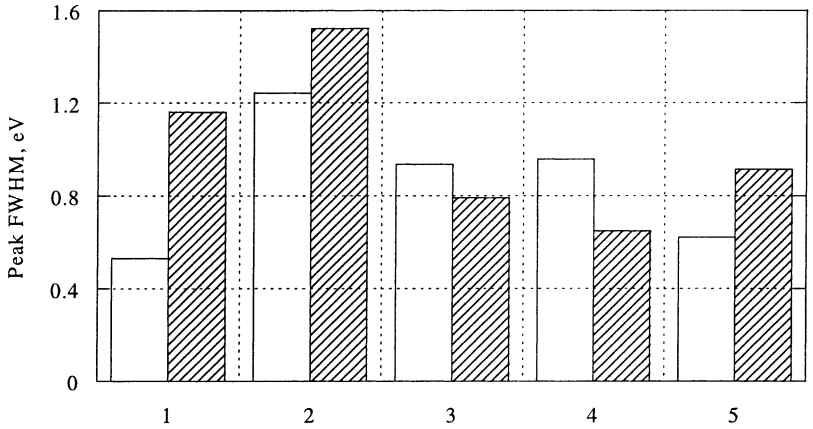

Fig. 5. XANES pre-edge peak widths for samples 1–5 (open bars: lower energy peak; hatched bars: higher energy peak).

and homogeneity. The shapes of the peaks appear to hold more substantial information. The presence of the alcohols in samples containing MAO raises peak height (compare samples 2 and 5, Fig. 3) and reduces peak width (Fig. 5). As with XPS, we assign this to increased site homogeneity.

3.3. EXAFS

To gain structural information on the catalyst samples, EXAFS analysis was performed using synchrotron XAS data acquired for the same samples described in Table 3. The *R*- and *k*-space spectra and fits for samples 1–5 are shown in Figs. 6–15. The EXAFS spectrum of sample 1 (Cp^*TiCl_3) was well fit with bond distances close to those for $Me_4EtCpTiCl_3$ [11]; an average Ti–C (Cp^* inner ring) distance of 2.405(7) Å was obtained by EXAFS versus 2.352(15) Å for the reference compound.

Even at the single-scattering level of analysis, reasonably good fits to the data for all four samples containing MAO were obtained using the same six shells: oxygen (one atom), aluminum (two atoms), and four shells of carbon, with two, five, six, and five atoms in each shell. Although (with rare exceptions [6]) connectivity among non-central atoms cannot be directly obtained from EXAFS data, the carbon shells

[6] These cases involve the use of multiple scattering or group scattering in accounting for spectral features.

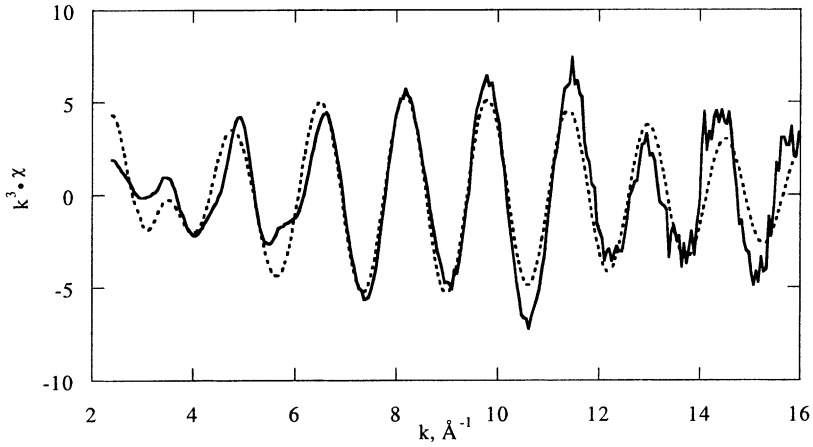

Fig. 6. Sample 1 EXAFS spectrum (solid line) and fit (dashed line). Fitting parameters: Ti–C (Cp*, inner ring) 2.405(7) Å; coordination no. 5; Debye–Waller factor (D–W) 0.004(2) Å^2. Ti–C (Cp*, outer ring) 3.39(6) Å; coordination no. 5; D–W 0.2(2). Ti–Cl 2.263(5) Å; coordination no. 3; D–W 0.006(1) Å^2. Goodness-of-fit parameter (R) = 42.8.

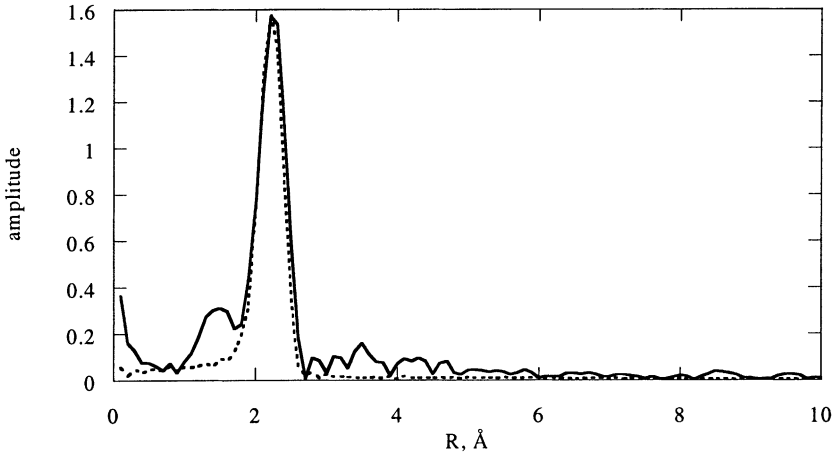

Fig. 7. Sample 1 EXAFS Fourier transform of experimental (solid line) and fit (dashed line) data.

for samples 2–5 are tentatively assigned as follows (see Table 4) — shell 2: Ti–CH_3; shell 4: Ti–$\mathbf{C}_5Me_5$; shell 5: Ti–arene; shell 6: Ti–$C_5\mathbf{Me}_5$. We are reasonably confident that the parameters obtained from these fits are statistically meaningful, despite the large number of shells.[7] Attempts at fitting the data to other sets of shells were less successful. In Table 5, the goodness-of-fit parameters are compared for the best-fitting four structures in Scheme 1, and it is clear that the combination of shells described above, shown as **IV** in Scheme 1, fits the data best. Structure **IV** is coordinatively saturated and, if cationic, formally bears 18 e$^-$ in its valence shell. In addition to the structures in Scheme 1 which failed to adequately fit the EXAFS data, the following formulae represent combinations of shells (excluding hydrogen atoms) for which the fitting routine could not even converge on a solution: Cp*$TiCl_n(CH_3)$; Cp*Ti(μ-CH_3)$_4Al_2$; Cp*Ti(CH_3)$_2$; Cp*Ti(CH_3)(η^1-ArO); Cp*Ti(CH_3)$_2$(η^6-C_6H_6); Cp*-

[7] Based on a k-space range of 14, an R-space range of 3 Å, and six shells, we obtain a ratio of $N_i/N_d = 27/19 = 1.42$, where N_i and N_d represent the number of independent and dependent fit parameters, respectively, see [12].

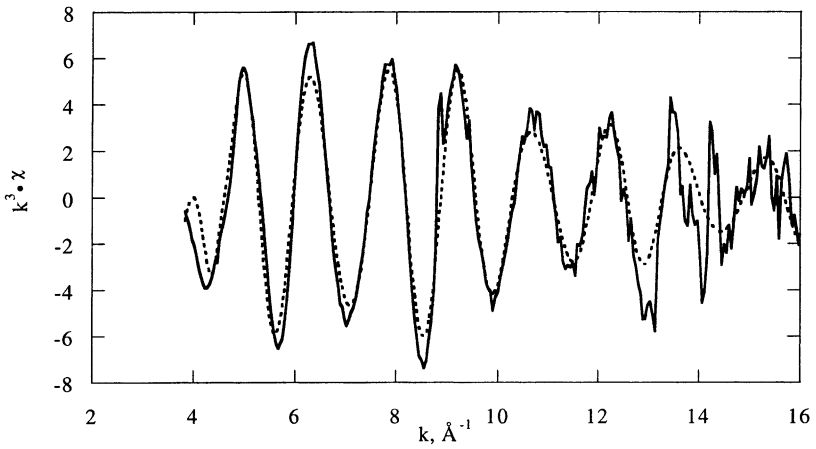

Fig. 8. Sample 2 EXAFS k^3-weighted spectrum (solid line) and fit (dashed line).

$Ti(CH_3)(\eta^1\text{-}ArO)(\eta^6\text{-}C_6H_6)$ (Ar = 2,6-di-*t*-butylphenyl). However, we must emphasize that, given the poverty of data in EXAFS relative to X-ray crystallography, the structure put forward is conjectural.

The Ti–O distance of 1.763–1.786 Å, though short, is not unusual for a covalent bond, and is similar to that seen in the crystal structure of $Cp^*Ti(OAr)Cl_2$ (Ar = 2,6-diisopropylphenyl) of 1.772(3) Å [7]. The oxygen may belong to either of the two alcohols, where present, or to MAO. However, it is difficult to imagine how the complex could simultaneously accommodate the bulky phenoxide, Cp^* ligand, and an η^6-arene ligand. A bridging oxo linkage to aluminum is offered here, mainly because it is consistent with the fact that sample 2 has no alcohols yet appears to have the same Ti–O moiety. The Ti–O–Al group could be formed through a ligand exchange reaction between Ti–Me and Al–O–Al units. The Ti–Cp^* (inner ring) distance of 2.301 Å derived from the fit of the EXAFS spectrum of sample 5 is considerably less than the average Ti–C (Cp^*) distance in the precursor. The shell assigned to methyl groups bound to titanium lies 2.1–2.2 Å from the central atom, a distance similar to that obtained for Cp^*TiMe_3 (2.107(5) Å) [13], yet it is

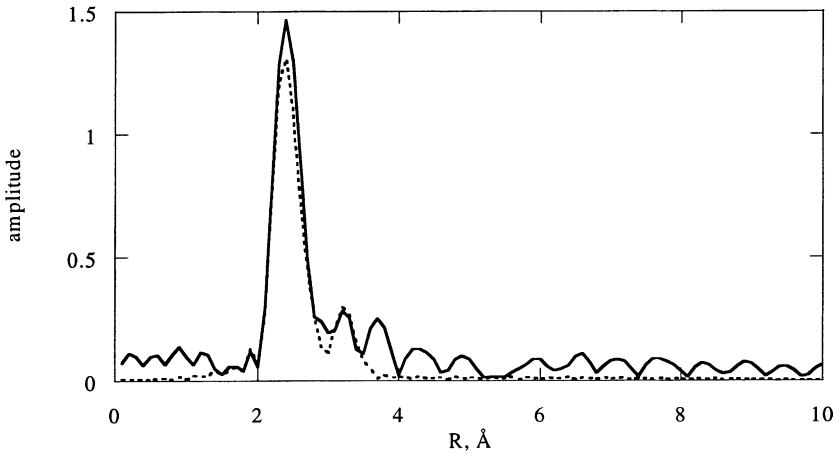

Fig. 9. Sample 2 EXAFS Fourier transform of experimental (solid line) and fit (dashed line).

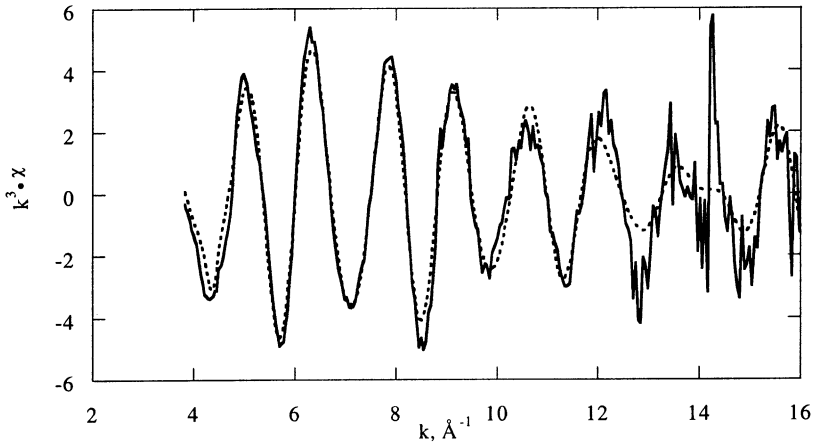

Fig. 10. Sample 3 EXAFS k^3-weighted spectrum (solid line) and fit (dashed line).

somewhat longer than the Ti–Me distance of 1.99(1) Å in the ionic species $[Cp^*_2Ti(CH_3)(THF)][BPh_4]$ [14]. The distances to Ti for the shells of aluminum atoms and the outer carbon ring of Cp* are not known with enough precision to permit much discussion. We will note that, while short, the distances from Ti to Al do not support direct bonding. It is almost certain that, if two Al atoms are in the sphere of non-bonded atoms near to Ti, that their distances to the central atom differ. We decided not to attempt fitting with additional shells for Al (or indeed for a non-symmetrically bound η^6-arene group) in order to minimize the number of fitting parameters while achieving a good fit. It must be emphasized as well that connectivity among the atoms surrounding the central atom (Ti) cannot be inferred from the single-scattering level of EXAFS analysis; therefore, the three-dimensional representations in Scheme 1 are to be seen as likely structures given the fit parameters.

The shell designated as an η^6-arene group is presumably due to the toluene used as solvent prior to drying, although it is possible that DTBP could provide a similar interaction in samples 4 and 5. Its distance to titanium of 2.68–2.72 Å is longer than expected. The closest structurally-characterized analogues of **IV** are $[Cp^*HfMe_2(MePh)][MeB(C_6F_5)_3]$

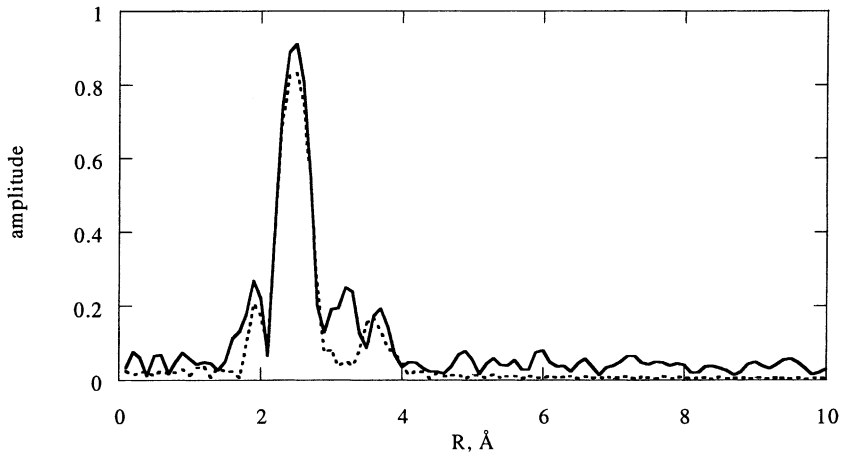

Fig. 11. Sample 3 EXAFS Fourier transform of experimental (solid line) and fit (dashed line).

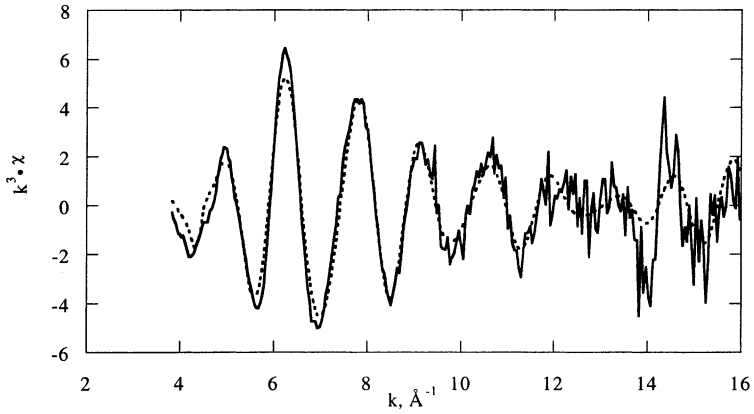

Fig. 12. Sample 4 EXAFS k^3-weighted spectrum (solid line) and fit (dashed line).

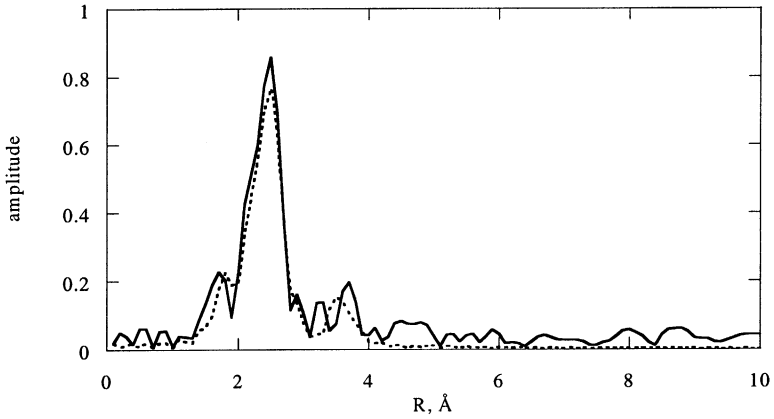

Fig. 13. Sample 4 EXAFS Fourier transform of experimental (solid line) and fit (dashed line).

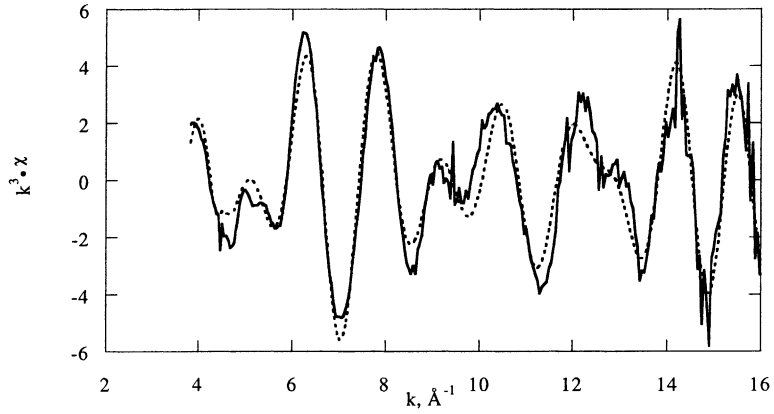

Fig. 14. Sample 5 EXAFS k^3-weighted spectrum (solid line) and fit (dashed line).

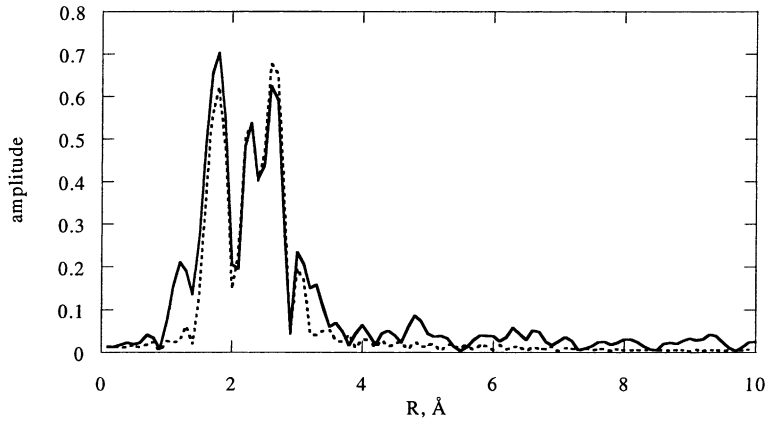

Fig. 15. Sample 5 EXAFS Fourier transform of experimental (solid line) and fit (dashed line).

Table 4
Structural parameters[a] from fits of EXAFS spectra of samples 2–5

Bond type[b]		Sample			
		2	3	4	5
Ti–O (CN = 1)[c]	R (Å)	1.784(12)	1.786(9)	1.763(8)	1.765(4)
	D–W[d] (Å^2)	0.10(9)	0.037(15)	0.015(5)	0.0004(6)
Ti–C (alkyl) (CN = 2)	R (Å)	2.22(4)	2.108(12)	2.15(4)	2.10(2)
	D–W (Å^2)	0.01(1)	0.005(2)	0.02(1)	0.020(6)
Ti–Al (CN = 2)	R (Å)	3.21(2)	3.62(2)	3.59(2)	2.99(3)
	D–W (Å^2)	0.01(2)	0.010(4)	0.011(4)	0.025(8)
Ti–C (**C**$_5$Me$_5$) (CN = 5)	R (Å)	2.316(6)	2.295(6)	2.291(8)	2.301(4)
	D–W (Å^2)	0.0004(8)	0.0040(8)	0.010(2)	0.007(1)
Ti–C (arene) (CN = 6)	R (Å)	2.722(14)	2.703(12)	2.701(13)	2.68(2)
	D–W (Å^2)	0.008(2)	0.009(2)	0.008(2)	0.032(8)
Ti–C (C$_5$**Me**$_5$) (CN = 5)	R (Å)	3.44(3)	3.45(3)	3.45(4)	3.44(3)
	D–W (Å^2)	0.11(9)	0.1(2)	0.1(2)	0.09(6)

[a] Values in parentheses represent 2σ limits in last digit of preceding number.
[b] CN values represent the coordination numbers used in fits. Features in boldface signify scattering shell within ligand.
[c] Coordination number, or number of atoms in the designated shell.
[d] Debye–Waller factor.

and [(1,3-(Me$_3$Si)Cp)HfMe$_2$(MePh)][MeB(C$_6$F$_5$)$_3$], with average Hf–C distances of 2.67 [15] and 2.69 Å [16], respectively. Given the smaller size of Ti, a Ti–C (arene) distance of about 2.52 Å would be predicted. [8]

Similarly, small values of 2.49–2.50 Å are given for the Ti(II) complexes (η^6-C$_6$R$_6$)Ti(AlCl$_4$)$_2$ (R = H [17], Me [18]). Considerable deviation from a symmetric η^6-arene interaction in **IV** is possible given the size of the Debye–Waller factors, and may explain the discrepancy. It is interesting to note that for several of the coordination shells, the bond lengths shorten as one or both alcohols are added to the composition. One interpretation of this observation is that there is

[8] The Hf–C (Cp*, inner ring) distance in [Cp*HfMe$_2$(MePh)][MeB(C$_6$F$_5$)$_3$] is 2.483 Å while we obtain a value of 2.301 Å for sample 5. This differential was applied to the Hf–C (arene) distance to obtain the expected value.

Table 5
Normalized qualities of fit (*R*-values) for samples 2–6, using model structures **I–IV** (see Scheme 1)

Structure	Sample			
	2	3	4	5
I	>60	>60	50.1	53.3
II	>65	>60	48.6	45.4
III	>60	40.8	53	47.5
IV	32.5	32.3	39.1	32.5

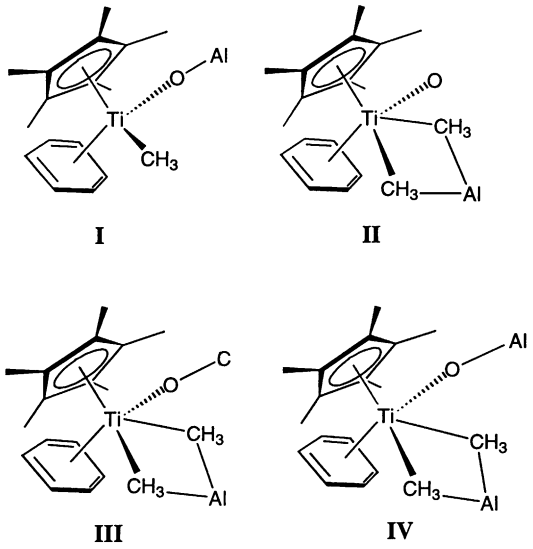

Scheme 1.

a higher proportion of reduced titanium species with longer bond lengths in sample 2 than in samples 3–5.

4. Conclusions

A new catalyst system for olefin polymerization, consisting of a combination of a half-sandwich titanium compound, MAO, and alcohol(s), has been found to exhibit high activity and a relatively high propensity to incorporate 1-hexene. The alcoholic components, particularly 2,6-di-*t*-butylphenol, appear to boost activity and limit the degree of catalyst heterogeneity. XPS and XANES analyses confirm that the average titanium center is more electron-poor when activated in the presence of methanol and/or DTBP; lineshape fitting leads to a conclusion that DTBP limits titanium site diversity. Detailed structural information has been obtained through analysis of the EXAFS spectrum of a catalyst sample containing Cp^*TiCl_3, MeOH, DTBP, and MAO reduced to solid form by vacuum drying of a toluene solution. Our tentative assignment of the average titanium environment includes, in addition to the η^5-C_5Me_5 ring, a short Ti–O bond, a Ti–(η^6-arene) interaction, as well as two bonds to alkyl carbon atoms. Interestingly, all samples made from Cp^*TiCl_3 and MAO, with or without MeOH or DTBP, appear to be fit best to the same structure as the four-component catalyst. If one accepts the assumption that in all samples, the titanium centers experience nearly the same average ligand environment, then the EXAFS fit parameters indicate a shortening of key bond distances, such as between titanium and oxygen atoms, in samples containing alcohols relative to the one lacking both.

The question of whether either alcohol is present in the coordination sphere of the active catalyst could not be conclusively resolved. Two sets of results, however, argue that neither alcohol is bonded directly to the metal center: (a) the polymerization data, which show that the same type of copolymer is formed in the absence of alcohol(s); (b) the EXAFS analysis, which shows that the titanium centers are surrounded by the same set of neighboring atoms whether the compositions include the alcohol(s) or not. If the activated catalyst is well-represented by **IV**, then atleast one ligand (most likely, that bearing the η^6-arene ring) must dissociate before an alkene molecule may coordinate to titanium and thus initiate polymerization.

Barring a direct alkoxide or aryloxide bond to titanium, how could the alcohol(s) influence the catalytic behavior of the Cp^*TiCl_3/MAO system? First, it could be argued that the alcohols react with trimethylaluminum, which is generally presented in MAO at levels up to 30 mol% (Al), thereby removing a strong reducing agent for titanium.[9] Second, one can imagine that the alcohol species, once assimilated into the cocatalyst structure as alkoxide units, might well tilt the equilibrium between tight and loose ion pairs toward the latter, and thus foster more rapid coordination and insertion of olefin. In the absence of more experimental data, these theories remain speculations.

[9] Note that in their polymerization examples, Nomura et al. [7] take pains to remove trimethylaluminum from MAO.

EXAFS analysis yields data which is by nature less concrete than those derived from other structural methods. In cases such as ours, where the active catalyst is formed through ligand exchange reactions with an amorphous cocatalyst, it is possibly the only means by which one can glean information of direct relevance to polymerization behavior.

Supporting information available

XANES spectra for samples 1–4. This material is available upon written request of the lead author.

Acknowledgements

The authors wish to thank Drs. M. Latimer and B. Hedman (SSRL) for assistance in acquiring XAS spectra and in the initial workup of the data. The following are acknowledged for their assistance in polymer characterization: B.J. Krantz (NMR), J. Karakowski (SEC), and J.E. Simborski (DSC). We thank D. Leder for assistance in catalyst analysis by XPS.

References

[1] S. O'Brien, J. Tudor, T. Maschmeyer, D. O'Hare, Chem. Commun. (1997) 1905.
[2] G. Zhang, P.R. Auburn, D.L. Beach, in: Proceedings of the 7th International Conference on X-ray Absorption Fine Structure, Kobe, Japan, 1992 (Jpn. J. Appl. Phys. 32 (Suppl. 32-2) (1993) 511).
[3] P. Andrews, J. Evans, J. Chem. Soc., Chem. Commun. (1993) 1246.
[4] D. Bogg, M. Conyngham, J.M. Corker, A.J. Dent, J. Evans, R.C. Farrow, V.L. Kambhampati, A.F. Masters, D.N. McLeod, C.A. Ramsdale, G. Salvini, Chem. Commun. (1996) 647.
[5] P.J. Ellis, R.W. Joyner, T. Maschmeyer, A.F. Masters, D.A. Niles, A.K. Smith, J. Mol. Catal. A: Chem. 111 (1996) 297.
[6] E.P. Wasserman, X. Bai, E.C. Fox, US Patent 5,962,362, filed 7 December 1997, to Union Carbide.
[7] K. Nomura, N. Naga, M. Miki, K. Yanagi, A. Imai, Organometallics 17 (1998) 2152.
[8] S. Bourgeois, P. le Seigneur, M. Perdereau, Surf. Sci. 328 (1995) 105.
[9] C.M. Greenlief, J.M. White, C.S. Ko, R.J. Gorte, J. Phys. Chem. 89 (1985) 5025.
[10] J.-M. Pan, B.L. Maschoff, U. Diebold, T.E. Madey, J. Vac. Sci. Technol. A 10 (1992) 2470.
[11] N.W. Alcock, G.E. Toogood, M.G.H. Wallbridge, Acta Cryst. Sect. C: Cryst. Struct. Commun. C40 (1984) 598.
[12] N. Binsted, R.W. Strange, S.S. Hasnain, Biochemistry 31 (1992) 12117.
[13] R. Blom, K. Rypdal, M. Mena, P. Royo, R. Serrano, J. Organomet. Chem. 391 (1990) 47.
[14] M. Bochmann, A.J. Jaggar, L.M. Wilson, M.B. Hursthouse, M. Motevalli, Polyhedron 8 (1989) 1838.
[15] D.J. Gillis, R. Quyoum, M.-J. Tudoret, Q. Wang, D. Jeremic, A.W. Roszak, M.C. Baird, Organometallics 15 (1996) 3600.
[16] S.J. Lancaster, O.B. Robinson, M. Bochmann, S.J. Coles, M.B. Hursthouse, Organometallics 14 (1995) 2456.
[17] U. Thewalt, F. Stollmaier, J. Organomet. Chem. 228 (1982) 149.
[18] U. Thewalt, F. Österle, J. Organomet. Chem. 172 (1979) 317.
[19] D. Briggs, M.P. Seah, Practical Surface Analysis by Auger and Photoelectron Spectroscopy, Wiley, New York, 1984.